03

Simulation of unsteady heat transfer and temperature separation on the blades of a gas turbine by changing the position of the nozzles of the combustion chamber

© D.K. Popova, N.N. Kortikov

Peter the Great Saint-Petersburg Polytechnic University,
195251 St. Petersburg, Russia
e-mail: daria_well96@mail.ru

Received October 11, 2023
Revised July 24, 2024
Accepted July 29, 2024

Using the URANS approach, a numerical model has been developed on the basis of which a decrease in temperature separation and dynamic loading on the turbine stage blades is predicted by changing the position of the injectors at the outlet of the combustion chamber. A decrease in the value of temperature separation (a decrease of 7.2% according to the time-averaged Nusselt number) and dynamic loading (a decrease of 81.6%) on the blade surface is possible by adjusting the position of the nozzle center relative to the entrance to the inter-blade channel of the nozzle block.

Keywords: rotor-stator interaction, unsteady heat transfer, temperature separation, clocking effect, dynamic loading.

DOI: 10.61011/TP.2024.10.59354.262-23

Introduction

Gas flow in turbo machines is unsteady in nature due to the gas-dynamic interaction of adjacent stationary and rotating arrays of blades (stator–rotor interaction) [1]. The subsonic potential interaction, shock wave interaction and wake interaction [2], and temperature non-uniformity at the combustion chamber outlet [3] are the main sources of unsteadiness in stator–rotor interaction.

The subsonic potential interaction arises as a result of mutual motion of stator and rotor blades and manifests itself in the form of unsteady pressure waves that propagate downstream and upstream and, consequently, alter periodically the kinematics of gas flow.

This unsteady potential interaction (propagation of pressure waves in the longitudinal direction) leads to a periodic variation of the thickness of the boundary layer and, accordingly, the intensity of a vortex wake behind the trailing edges of blades. If the flow becomes supersonic in the region of the trailing edge of a blade, the forming system of shock waves will interact with the inlet blade edge downstream, increasing the amplitude of pressure pulsations.

It was established experimentally [4] that the non-uniformity of the temperature field at the nozzle array entrance (combustion chamber outlet) affects the thermal loading of rotor blades: the flow is segregated (separated) in the rotor inter-blade channels, and „hot“ layers move to the surface of the pressure side , while „cold“ layers move to the surface of the suction side.

The first qualitative explanation of this effect (temperature separation) has been provided in [5] and involves the analysis of the velocity triangle in the turbine stage (Fig. 1). The notation in the figure is as follows: V — absolute velocity, W — relative velocity, ω — vorticity vector, Ω — angular velocity, and R — radius; subscripts: hot — hot gas, cold — cold gas, n — normal projection, and s — tangential projection.

Thus, with reduced gas velocities at the nozzle block outlet being equal, the regions with a higher temperature should have a higher absolute velocity Vhot than those with a lower temperature ($V_{\text{hot}} > V_{\text{cold}}$) at constant relative velocity ($W_{\text{hot}} = W_{\text{cold}}$). This will reduce the angle by $\Delta\alpha$ (i.e., lead to an increase in the angle of attack and a shift of hot gas to the trough of a working blade; see Fig. 1, *a*). In a similar fashion, cold gas may shift to the back. Owing to this, the time-averaged temperature

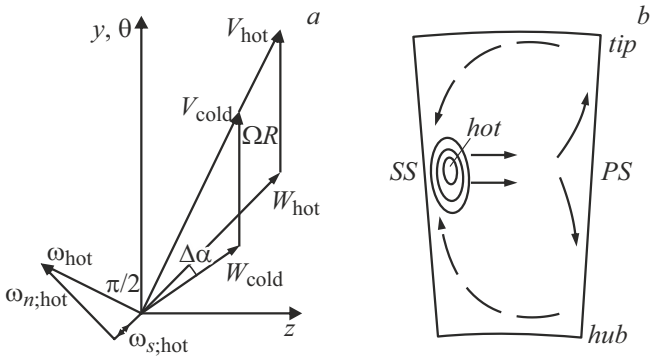

Figure 1. Diagrams of velocity (*a*) and vorticity (*b*) triangles at the stator/rotor interface [5].

of the pressure side exceeds the temperature of the back.

It was noted in [6,7] that temperature separation is associated quantitively with the processes caused by periodic unsteadiness and mass forces (centrifugal forces and the Coriolis force), which have the capacity to generate three-dimensional secondary flows (Fig. 1, *b*).

As a result, hot gas on the pressure side (PS) spreads from the middle of the channel to the hub and the periphery, which leads to heating of the upper and lower walls. On the convex side (SS), cold gas flows from the end wall to the middle of the channel.

The features of transfer of temperature non-uniformity in the flow passage of the stage in relation to the circumferential position of the heat spot at the entrance to the turbine stage (*clocking effect*) were examined in [8]. It was noted in these studies that the temperature state and the amplitude-frequency spectrum of the flow around a working blade (dynamic loading) may be altered by adjusting the circumferential position of the injector at the combustion chamber outlet relative to the inlet edge of a nozzle blade.

In [9], a „hot streak“ (heat spot) was positioned at four sites along the circumference, which corresponded to different positions of the spot relative to the inlet edge of a nozzle blade. The results of measurements of the temperature and total pressure fields in the flow passage of the stage revealed that this circumferential shift of the injector has only a weak influence on the total pressure losses. At the same time, the shift had a noticeable effect on the vorticity field (intensifying it) and the unsteady thermal load on a working blade of the turbine stage.

It was demonstrated that a dramatic deformation of the hot streak may be induced by directing the hot spot at the inlet edge of a nozzle blade. The worst possible operating conditions for a nozzle blade are established when the hot spot is at its inlet edge. It was noted that the hot spot positioning in the middle of the span between injectors guarantees the least interaction with the inlet edge and maximizes temperature diffusion in the flow passage.

The combined effect of flow swirl and the temperature spot positioning at the stage entrance on the unsteady gas flow in the impeller was examined in [10,11]. The results of amplitude-frequency analysis of numerical calculation data revealed that the maximum amplitude of flow oscillation in the flow passage of the impeller corresponds to the fundamental frequency of the turbine stage.

The direction (sign) of swirl affects the course of unsteady processes: the amplitude of oscillation of thermal load on the surface of a working blade with positive swirl is 40% greater than with negative swirl.

The authors of [12] did not limit themselves to studying the influence of temperature non-uniformity at the stage entrance on the integral characteristics of the turbine stage only (namely, the thermal and power loads). They used a conjugate approach to numerical modeling of the temperature state of a working blade under convective film cooling. This formulation allows one to determine local overheating of metal of the blade profile.

However, no detailed studies of the temperature separation effect have been conducted; only a reduction of the adiabatic temperature of the trailing edge by 24 K with a 10% displacement of the hot spot toward the trough was mentioned.

The LES (large eddy simulation) approach was used in [13] in the analysis of interaction in the „combustion chamber–nozzle block“ system at a single position of the injector relative to the turbine stage entrance. The features of rotor–stator interaction with non-uniformity of the input temperature were not analyzed.

The aim of the present study is to model numerically and analyze the unsteady gas-dynamic and thermal phenomena in a turbine stage with inlet temperature non-uniformity and use the obtained results to examine the influence of circumferential shift of the combustion chamber injectors (clocking effect) on temperature separation and dynamic loading on working blades of the turbine stage.

1. Problem formulation and computational aspects

The calculation of gas-dynamic processes in a turbine stage was performed in the STAR CCM+ software package (17.06.007-R8) [14] in the three-dimensional formulation. The system of Reynolds-averaged Navier–Stokes equations characterizing unsteady flow of a perfect compressible gas with a variable dynamic viscosity (Sutherland's law) and variable heat capacity and thermal conductivity was solved. The Menter k–ωSST turbulence model with a correction for the curvature of streamlines was chosen. The coupled solver with second-order accuracy was used.

The computational domain has two regions: one interblade channel in the stator region and two channels in the rotor region (Fig. 2). The LPI stage [15,16] features 24 nozzle blades ($Z_S = 24$) and 48 working blades ($Z_R = 48$). The stagnation inlet (stagnation pressure and temperature) boundary condition was set at the turbine entrance. The

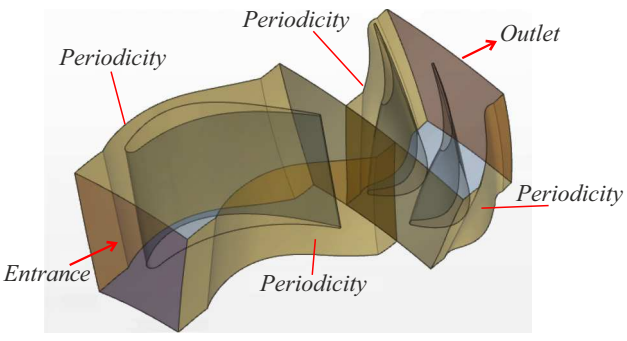

Figure 2. Computational domain.

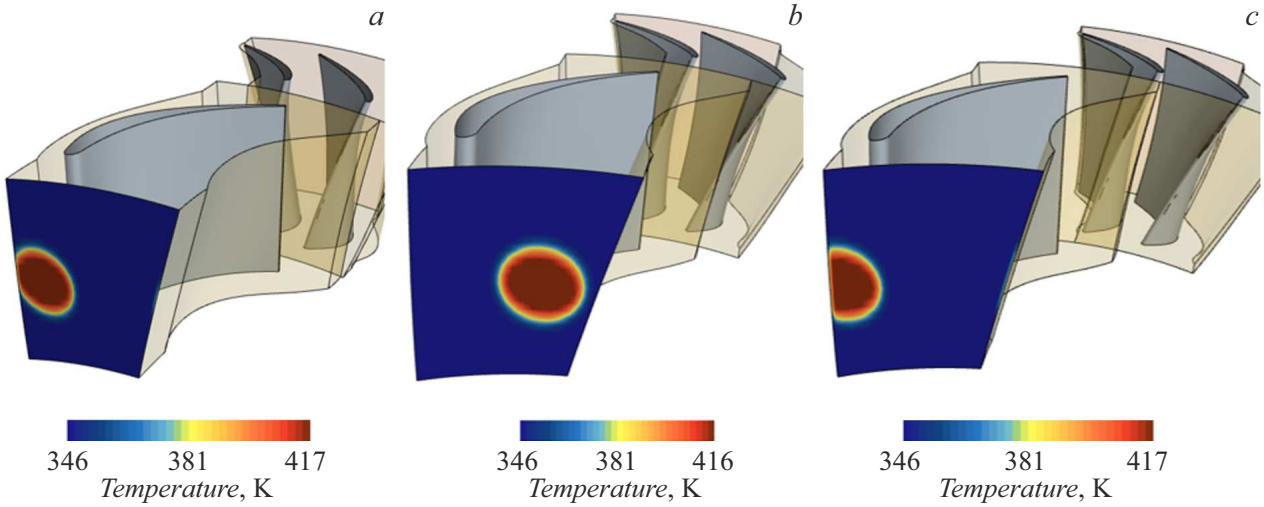

Figure 3. Positioning of injectors relative to the nozzle block: *a* — near the pressure side (*PS*); *b* — in the center of the inter-blade channel (*CC*); *c* — near the suction side (*SS*).

pressure outlet condition was set at the outlet of the computational domain. The periodicity condition was set at the lateral boundaries of regions. A constant temperature of $T = 500\,\mathrm{K}$ was specified for the surfaces corresponding to the feather of a working blade; all the other solid surfaces were considered to be adiabatic.

Three positions of injectors of the combustion chamber relative to the inter-blade channel of the nozzle block were considered: the center of an injector could be located near the pressure side (*PS*), at the center of the inter-blade channel (*CC*), or near the suction side (*SS*). The center of the heat spot in Fig. 3 is on the injector axis.

The non-uniformity o stagnation temperature at the entrance to the stage is represented as a cylindrical region with its inner boundary having a temperature of $T = 420\,\mathrm{K}$ if $r \leq 0.01$; the outer boundary has $T = 350\,\mathrm{K}$ if $r \geq 0.015$. In the $0.01 \leq r \leq 0.015$ transition region, conjugation in the temperature pattern is established by a third-order polynomial. The total pressure at the stage entrance is $P^* = 1.4\,\mathrm{bar}$, and the static pressure at the stage outlet is $P = 1\,\mathrm{bar}$.

The kinematic and operating parameters of the LPI turbine stage are similar to the corresponding characteristics of the *ACE* stage [17]. Therefore, the calculation model was validated with the experimental data for this stage at the following values of similarity parameters: Reynolds number $\mathrm{Re} = \frac{Vl}{\nu} = 3.4 \cdot 10^5$; Strouhal number $Sh = \frac{fl}{V} = 1.05$; rotary parameter $K = \frac{\omega d_{eq}}{w} = 0.12$; and temperature non-uniformity $\mathrm{TD} = 0.14$ equal to the ratio of the difference between the maximum and average temperatures to the temperature difference in the combustion chamber, where V is the characteristic velocity, [m/s], l is the chord length of a working blade, [m], ν is the kinematic viscosity, [m^2/s], f is the fundamental frequency of the nozzle block, [Hz], ω is the angular velocity of the impeller rotation, [rps], d_{eq} is the equivalent diameter of the flow passage of the impeller, [m], and w is the relative angular flow velocity, [m/s].

The base computational grid contained approximately 1.3 million prismatic cells, and the typical values of y^+ in the first wall cell do not exceed 5. The results of preliminary studies of grid convergence demonstrated that further grid refinement is impractical.

2. Comparison of calculated and experimental data

Figure 4 presents a comparison of the numerical calculation results and the experimental data from [17] for the variation of thermal flow density on the blade surface (in the central height section) with time at monitoring Point 1. A satisfactory agreement is evident (the uncertainty, which was calculated as the difference between the calculation results and the experimental data divided by the experimental values, does not exceed 10%).

Dimensionless time scaled by the time needed for a working blade to travel in the circumferential direction from the center of an injector to the center of the next one is plotted on the abscissa axis.

Figure 5 shows the distribution of calculated and experimental data on time-averaged heat exchange along the outline of a working blade. Calculated data obtained under constant and variable thermal conductivities are presented. The outline of a working blade (abscissa axis) is a dimensionless arc coordinate normalized to the chord of the blade.

The model with a variable thermal conductivity (with a third-order polynomial dependence on temperature) provides a better result (round dots) than the calculation with

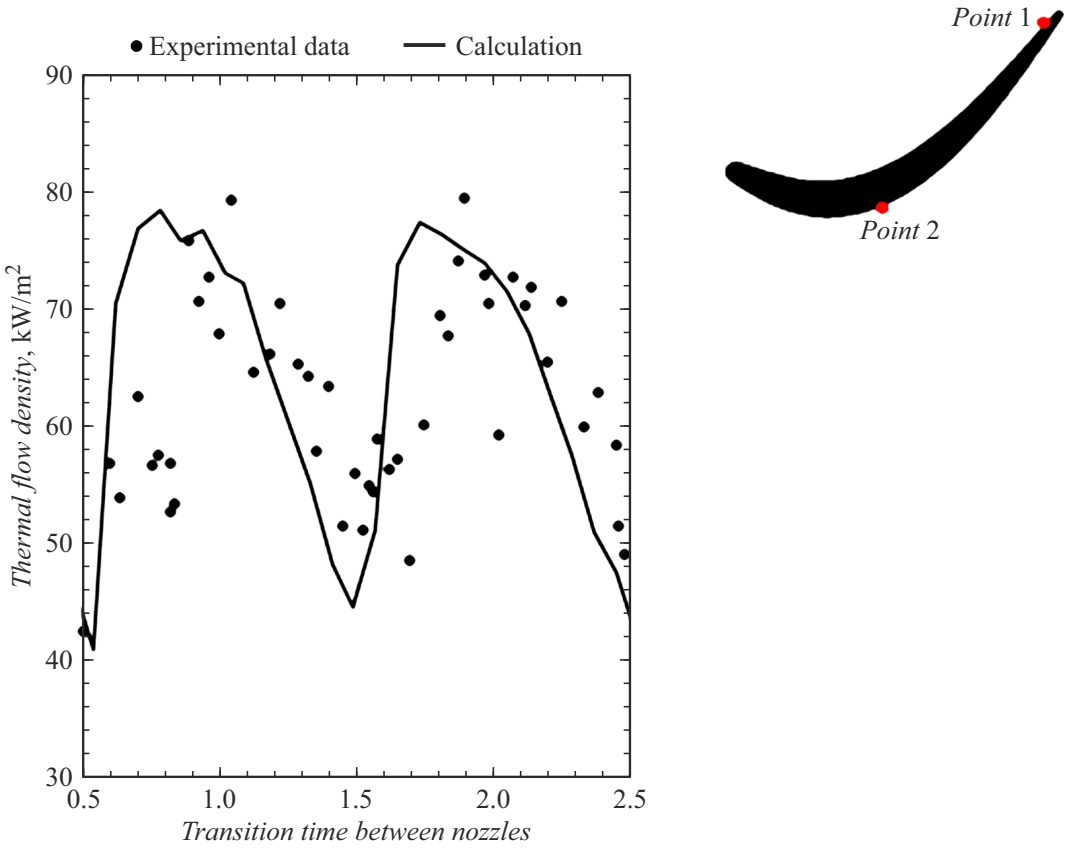

Figure 4. Variation of thermal flow density on the surface of a working blade (calculated and experimental data [17]).

a constant thermal conductivity (solid curve in Fig. 5). This is evidenced by a monotonic distribution of the local heat transfer coefficient on the back of a blade, which is typical of the unseparated flow regime. In addition, the model with a variable thermal conductivity provides a closer fit between the calculated and experimental data for the trough part of the blade profile.

3. Temperature separation control

The generation of three-dimensional secondary flows spreading from the middle of the channel to the hub and the periphery under the influence of mass forces was noted at all the examined injector positions (Fig. 6). The intensity of secondary flows is at its minimum when the injector is located at the center of the inter-blade channel of the nozzle block [6,7].

Figure 6 (a fragment in the form of a temperature isosurface on the right) illustrates this case by presenting the structure of a heat jet and its interaction with a working blade.

The heat balance equation for a flat wall with the boundary conditions of the third kind with different values of the heat transfer coefficient of the back and trough (α_{back} and α_{trough}) was used to obtain an expression for the ratio of temperatures on the opposite surfaces of a plate:

$$\frac{t_{trough}}{t_{back}} = \frac{1 + Bi\left[1 + \frac{t_g}{t_{back}}\left(\frac{\alpha_{trough}}{\alpha_{back}} - 1\right)\right]}{\left(1 + Bi \cdot \frac{\alpha_{trough}}{\alpha_{back}}\right)},$$

$$Bi = \frac{\alpha_{back}\delta}{\lambda}. \quad (1)$$

Here, Bi is the Biot number, t is temperature, [°C], α is the coefficient of heat transfer from the body surface to the environment, [W/(m^2 · K)], δ is the thermal conductivity coefficient of the body material, [W/(m·K)], and δ is the characteristic size (thickness) of the solid body, [m]; subscript g denotes gas.

The Biot number for the material of aircraft turbine blades under real operating conditions is 0.2 [18]. The ratios (averaged over the blade surface) of Nusselt numbers and temperatures at the pressure side and back calculated by formula (1) for three different injector positions are listed in the table.

The effect of temperature separation is minimized when the injector is located at the center (CC) of the inter-blade channel of the nozzle block. The results of spectral analysis of unsteady thermal flow at monitoring points on the trough (Point 1) and the back (Point 2) are presented in the form of an amplitude-frequency characteristic in Fig. 7. The

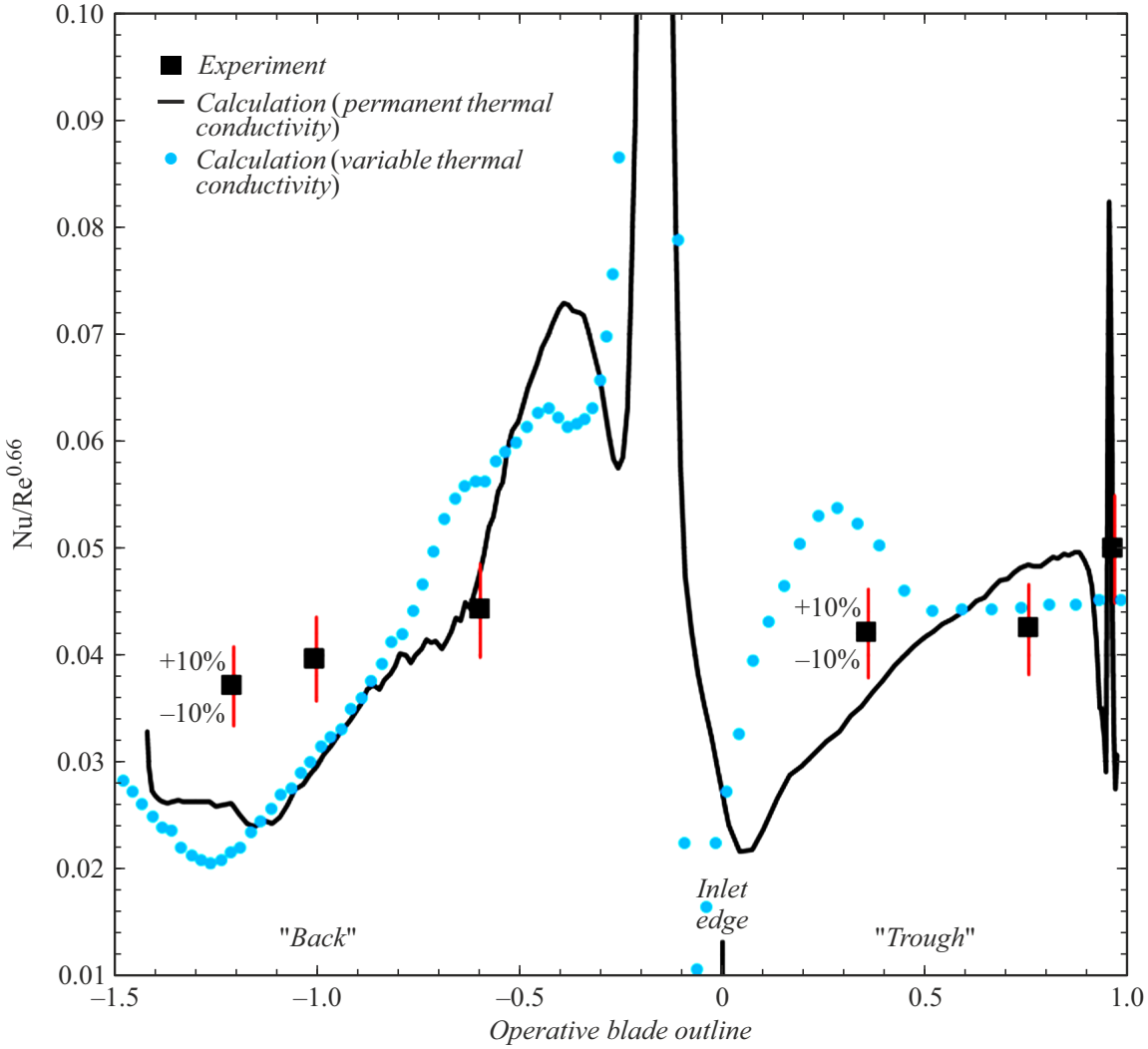

Figure 5. Heat exchange on the surface of a working blade in the central height section (injector opposite the inlet edge of a nozzle blade). (Calculated and experimental data [17]).

fundamental frequency of flow excitation (due to rotation of the working array) is $f_s = \frac{5000\text{rpm}}{60} \cdot Z_R = 4.0\,\text{kHz}$ for the nozzle array and $f_R = 2.0\,\text{kHz}$ for the working array.

The calculations revealed that the dominant peak in the intensity of thermal flow oscillations on blade surface S is the fundamental frequency of 2.0 kHz. The next intensity peaks are 5 and 10 times lower than the dominant value and are observed at multiples of the fundamental frequency (4.0 and 6.0 kHz, respectively).

The clocking effect affects the amplitude of thermal flow oscillations on the surface of a working blade. The injector positioning at the center of the inter-blade channel of the nozzle array (CC1 and CC2, Fig. 7) minimizes the dynamic loading (oscillatory additive to the thermal flow).

In turn, a shift of the injector center toward the suction surface (the back of s nozzle blade; SS1 and SS2 in Fig. 7) contributes to an increase in dynamic loading. An intermediate loading level is obtained when the injector is shifted toward the nozzle pressure side (PS1 and PS2).

In addition, the amplitude-frequency characteristic verifies the validity of application of the URANS approach in the present problem. The range of frequencies reproduced adequately by the URANS numerical solution is extremely narrow. The URANS method is not designed to reproduce the real spectrum of turbulent pulsations. It is used to simulate large-scale periodic flow pulsations [19]. The frequencies of turbulent pulsations in such problems range from 7 to 35 kHz [17] and are significantly higher than the characteristic frequencies presented in Fig. 7.

Conclusion

Both the development of mathematical models and the selection of design parameters (of which the injector

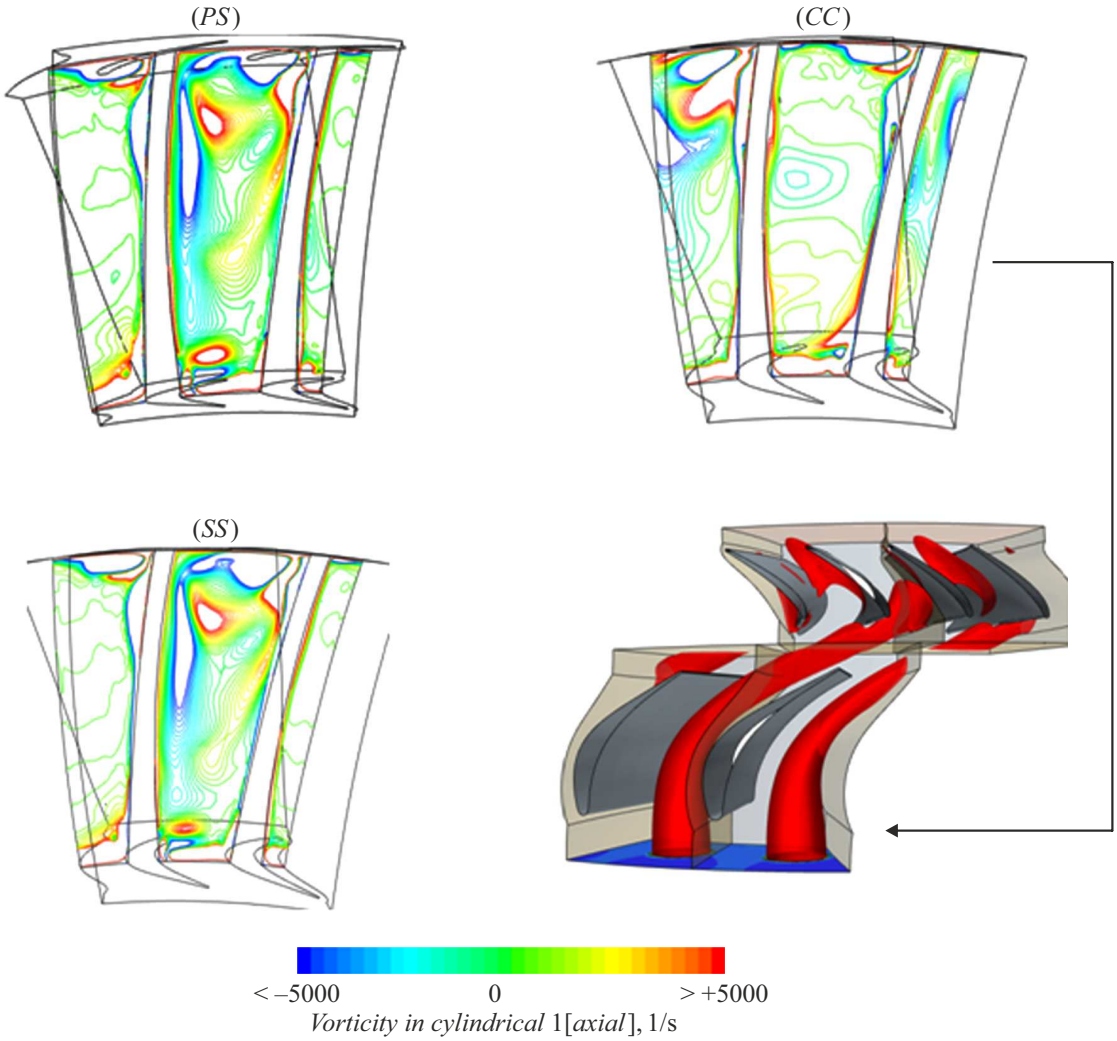

Figure 6. Isolines of the longitudinal vorticity vector component and isosurface of a heat jet.

Temperature separation magnitude as a function of injector positioning

	PS	*SS*	*CC*
Nu_{trough}/Nu_{back}	1.49	1.42	1.39
t_{trough}/t_{back}	1.026	1.023	1.021

position is an example) providing the required performance levels of the modeled system are major problems in construction of advanced and competitive equipment.

The results of numerical modeling revealed a suppression of temperature separation (by 7.2% in the Nusselt number) and dynamic loading (by 81.6%) on the surface of a working blade when the injector was positioned centrally relative to the entrance to the inter-blade channel of the nozzle array.

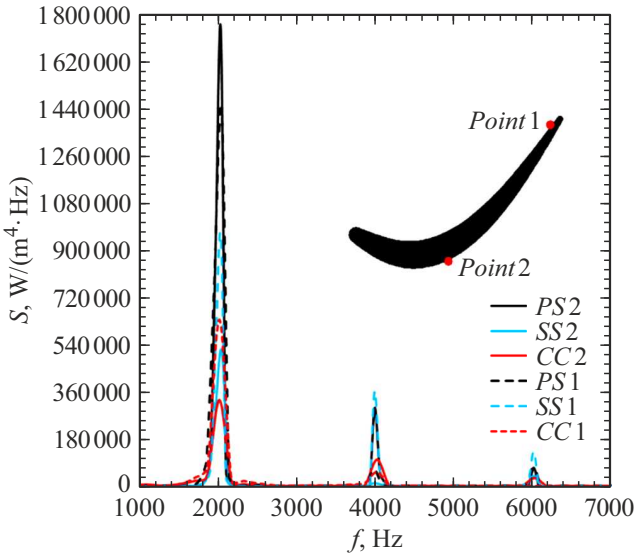

Figure 7. Amplitude-frequency characteristic of unsteady thermal flow.

Conflict of interest

The authors declare that they have no conflict of interest.

References

[1] G.S. Samoilovich. *Nestatsionarnoe obtekanie i kolebaniya lopatok v turbomashinakh* (Nauka, M., 1969) (in Russian).

[2] V.G. Avgustinovich, Yu.N. Shmotin. *Chislennoe modelirovanie nestatsionarnykh yavlenii v gazoturbinnykh dvigatelyakh* (Mashinostroenie, M., 2005) (in Russian).

[3] T. Shang, A.H. Epstein. ASME J. Turbomachinery, **119** (7), 543 (1997).

[4] A.P. Saxer, H.M. Fend. *Numerical Analysis of 3-D Unsteady Hotstreak Migration and Shock Interaction in Turbine Stage* (International Gas Turbine and Aeroengine Congress and Exposition The Hague, Netherlands — June 13–16, 1994), 12 p.

[5] T. Shang, G.R. Guenette, A.H. Epstein, A.P. Saxer. *The Influence of Inlet Temperature Distortion on Rotor Heat Transfer in a Transonic Turbine.* (31st AIAA/ASME/SAE/ASEE. Joint Propulsion Conference and Exhibit, 1995), AIAA 95-304, 11 p.

[6] B.T. An, J.-J. Liu, H. De Jiang. ASME J. Turbomachinery, **131**, 031015 (2009).

[7] A.M. Basol, P. Jenny, M. Ibrahim, A.I. Kalfas, R.S. Abhari. J. Eng. Gas Turbines Power, **133**, 061901 (2011).

[8] J. Ong, R.J. Miller. ASME J. Turbomachinery, **134**, 051002 (2012).

[9] P. Gaetani, G. Persico. *Hot Streak Evolution in an Axial HP Turbine Stage* (Proceed. 12th Europ. Conf. Turbomachinery Fluid dynamics & Thermodynamics ETC12, Stockholm, Sweden, 2017), 14 p.

[10] B. Khanal, L. He, J. Northall, P. Adami. *Unsteady Aerothermal Behavior of HP Turbine Stage Under Influence of Combustor hot Streak and Swirl* (Proceed. ISUAAAT. ISUAAAT–18–59-1. 2013), 9 p.

[11] M.G. Adams, P.F. Beard, M.R. Stokes, F. Wallin, K.S. Chana, Th. Povey. ASME J. Turbomachinery, **143**, 021011 (2021).

[12] D. Griffini, M. Insinna, S. Salvadori, F. Martelli. ASME J. Turbomachinery, **138**, 021006 (2016).

[13] C. Koupper, G. Bonnau, L. Gicquel, F. Duchaine. *Large Eddy Simulations of the Combustor Turbine Interface: Study of the Potential and Clocking Effects* (Proceed. ASME Turbo Expo 2016: Turbomachinery Technical Conference and Exposition. GT2016-56443), 12 p.

[14] Simcenter STAR-CCM+ 2022.1 User Guide. 10756 p.

[15] A.V. Grigoriev, A.I. Iakunin, N.B. Kuznechov, V.F. Kondratiev, N.N. Kortikov. *Application of Harmonic Balance Method to the Simulation of Unsteady Rotor/Stator Interaction in the Single Stage* (Proceed. 10th Europ. Conf. Turbomachinery. Fluid Dynamics & Thermodynamics. ETC10, 2013, Lappearanta. Finland), p. 854–864.

[16] N. Kortikov. *Simulation of the Joint Effect of Rotor-Stator Interaction and Circumferential Temperature Unevenness on Losses in the Turbine Stage* (MATEC Web of Conf. 2018. 245. 04006),
DOI: 10.1051/matecconf/201824506008 EECE-2018

[17] T. Shang. *Influence of Inlet Temperature Distortion on Turbine Heat Transfer* (PhD diss., Massachusetts Institute of Technology, 1995), 224 p.

[18] A.V. Shchukin, A.V. Il'inkov, V.V. Takmovtsev, T.A. Il'inkova, I.I. Khabibullin. *Teplofizika rabochikh protsessov v okhlazhdaemykh lopatkakh gazovykh turbin* (KNITU-KAI, Kazan', 2020) (in Russian).

[19] A.Yu. Snegirev. *Vysokoproizvoditel'nye vychisleniya v tekhnicheskoi fizike. Chislennoe modelirovanie turbulentnykh techenii: uchebnoe posobie* (Izd. Politekh. Univ., SPb., 2009) (in Russian).

Translated by D.Safin